Cancer Research

Optimizing a Lupus Autoantibody for Targeted Cancer Therapy

Philip W. Noble[1], Grace Chan[2], Melissa R. Young[1,3], Richard H. Weisbart[2], and James E. Hansen[1,3]

Abstract

The specificity of binding by antibodies to target antigens is a compelling advantage to antibody-based cancer therapy, but most antibodies cannot penetrate cells to affect intracellular processes. Select lupus autoantibodies penetrate into cell nuclei, and the potential for application of these antibodies in cancer therapy is an emerging concept. Here, we show that a divalent lupus anti-DNA autoantibody fragment with enhancing mutations that increase its ability to penetrate cell nuclei and bind DNA causes accumulation of DNA double-strand breaks in and is highly and selectively toxic to cancer cells and tumors with defective homology-directed repair of DNA double-strand breaks. These findings provide proof of principle for the use of optimized lupus autoantibodies in targeted cancer therapy. *Cancer Res; 75(11); 2285–91. ©2015 AACR.*

Introduction

Rational design of targeted cancer therapies requires development of safe and specific modulators of tumor targets. The unrivaled specificity of binding by antibodies to their antigens gives them a compelling therapeutic advantage over other molecules that have significant off target effects. However, most antibodies do not cross plasma membranes and cannot directly affect intracellular processes. Select lupus autoantibodies have the unusual capacity to penetrate into cells, and we now recognize a potential new paradigm in antibody-based cancer therapy in which cell-penetrating lupus autoantibodies are used to disrupt key intracellular processes to selectively affect cancer cells. The nuclear-localizing lupus anti-DNA autoantibody 3E10 is the prototype that exemplifies this approach. 3E10 penetrates into cell nuclei, binds DNA, and inhibits both base excision repair (BER) and homology-directed repair (HDR) of DNA double-strand breaks (DSB; ref. 1). The degree to which 3E10 inhibits these DNA repair pathways is not sufficient to kill normal cells, but cancer cells with preexisting defects in HDR due to BRCA2 deficiency are somewhat sensitive to 3E10 (1). These findings revealed the potential to apply 3E10 as a targeted therapy for HDR-deficient tumors. However, an optimized 3E10 derivative with increased effect on HDR-deficient cancer cells is needed to allow translation of this discovery into a clinically relevant therapy.

In seeking to optimize 3E10 for targeted therapy of HDR-deficient malignancies, we have chosen to focus on 3E10 fragments that are missing Fc regions and carry less risk of nonspecific Fc-mediated activation of complement or antibody-dependent cell-mediated cytotoxicity (ADCC). A 3E10 single-chain variable fragment (hereafter referred to as scFv) that lacks an Fc region and has a D31N mutation in the V_H region of the first complementarity determining region (CDR1) has previously been generated (2, 3). The D31N mutation significantly increases the DNA-binding affinity and efficiency of nuclear penetration by scFv, but despite this scFv still has only a modest effect on BRCA2-deficient cancer cells (1). We set out to build a more potent 3E10 fragment based on the scFv platform.

The primary two biochemical terms used to describe the quality of interaction between an antibody and its target antigen are the binding affinity and avidity. Affinity specifically quantifies the strength of the interaction between a single antigen–binding domain and the target antigen. Avidity, by contrast, refers to the strength of the overall interaction between the antibody and the antigen, and takes into account the exponential improvement in binding afforded by the presence of multiple antigen–binding sites in multivalent antibodies (4). The binding affinity of scFv to DNA has already been enhanced by the D31N mutation, but because scFv possesses only a single DNA–binding domain there remains room to build on the fragment's binding avidity. It has previously been established that multivalent antibody fragments bind with much greater avidity to target antigens compared with monovalent fragments (5, 6), and we therefore hypothesized that a divalent 3E10 fragment with D31N mutations would have significantly increased avidity for DNA compared with scFv, and therefore yield more efficient accumulation of DNA damage in and have a more potent impact on the survival of HDR-deficient cancer cells. To test this hypothesis, a 3E10 di–single-chain variable fragment with D31N mutations (hereafter referred to as di-scFv) was generated and evaluated for potential as a targeted therapy for HDR-deficient malignancies.

Materials and Methods

Recombinant proteins

ScFv was generated as previously described (1). Di-scFv, a 3E10 di–single-chain variable fragment with D31N mutations, was

[1]Department of Therapeutic Radiology, Yale School of Medicine, New Haven, Connecticut. [2]Department of Research, Veterans Affairs Greater Los Angeles Healthcare System, Sepulveda, California. [3]Yale Cancer Center, Yale School of Medicine, New Haven, Connecticut.

Corresponding Author: James E. Hansen, Yale School of Medicine, 15 York Street, HRT 142, New Haven, CT 06520. Phone: 203-737-4429; Fax: 203-785-3023; E-mail: james.e.hansen@yale.edu

doi: 10.1158/0008-5472.CAN-14-2278

generated by recombinant fusion of two scFv fragments. Intervening linker sequences were placed between scFv segments in di-scFv as previously described (7). cDNA-encoding di-scFv was ligated into the *pPICZαA* yeast expression vector, and *pPICZαA-di-scFv* was transfected into X-33 cells. Di-scFv was expressed in and purified from X-33 supernatant using the techniques as previously described (8–10). Protein concentrations were determined by UV spectrophotometry using a NanoDrop 1000 (Thermo Fisher Scientific). Typical final yield of purified di-scFv from a 1 L culture was 1 mg.

Cell lines

H1975, HCT116, SW48, and the matched pair of isogenic BRCA2-proficient and -deficient DLD1 colon cancer cells were obtained from Horizon Discovery Ltd., which performs cell line validation by short tandem repeat profiling. PTEN-deficient U251, U251 transfected with a tetracycline-inducible PTEN expression vector system (U251-PTEN), and BRCA2-deficient CAPAN-1 cells were a gift from Peter Glazer. U251 and U251-PTEN cell lines were grown in DMEM (Life Technologies) supplemented with 10% FBS (Sigma-Aldrich). PTEN expression was induced in U251-PTEN with the addition of 400 μg/mL G418, 2 μg/mL blasticidin, and 1 μg/mL doxycycline. All other cell lines were grown in RPMI-1640 (Life Technologies) supplemented with 10% FBS.

Cell-penetration assays

DLD1 cells grown in 96-well plates were treated with control buffer or 5 μmol/L scFv or di-scFv for 1 hour at 37°C. Cells were then extensively washed with PBS, fixed with chilled 100% ethanol for 5 minutes, washed again with PBS, and then probed with an anti-Myc antibody (clone 9E10) overnight at 4°C. Cells were then washed and then probed with Alexa488-conjugated goat anti-mouse IgG antibody for 1 hour at 4°C (Cell Signaling Technology). Cells were then washed and counterstained with propidium iodide (PI; Sigma-Aldrich) for 30 minutes at room temperature to allow visualization of cell nuclei. Nuclear penetration by the antibodies and PI staining was then imaged using an EVOS fl digital fluorescence microscope (Advanced Microscopy Group) using GFP and red fluorescent protein (RFP) filters (×40 magnification; Life Technologies). GFP and RFP images were merged using ImageJ (NIH, Bethesda, MD).

γH2AX and phospho-53BP1 foci

U251, U251-PTEN, and CAPAN-1 cells were allowed to adhere to glass coverslips overnight at 37°C prior and then treated with control buffer, scFv, or di-scFv. Cells were then incubated at 37°C for 4 or 24 hours and then washed with PBS before fixing with 4% formaldehyde in PBS at 4°C for 15 minutes. Cells were next washed again and then blocked with 5% goat serum diluted in PBS with 0.3% Triton X-100 for 60 minutes at 4°C. Cells were then incubated overnight at 4°C with either anti-γH2AX or anti–phospho-53BP1 (Ser1778) antibodies (Cell signaling Technology). Cells were subsequently washed and probed with Alexa 555–conjugated goat anti-rabbit IgG (H+L; Life Technologies) for 60 minutes at 4°C. Next, cells were washed with PBS and mounted onto microscope slides with ProLong Gold Antifade reagent with DAPI for nuclear counterstaining (Cell Signaling Technology). Slides were cured for 24 hours in the dark before imaging using an Axiovert 200 microscope (Carl Zeiss MicroImaging, Inc.). Mean number of foci per cell was determined from counts in at least 100 cells per condition.

Clonogenic survival assays

Surviving fractions of cells treated with control media or media containing scFv or di-scFv were determined by colony formation assay as previously described (1).

CAPAN-1 tumor study

CAPAN-1 tumors were established in athymic (NCr nu/nu) male mice ages 5 to 6 weeks by s.c. injection of 5×10^6 CAPAN-1 cells in the right flank. Sixteen mice were injected with tumor cells, and tumors with consistent growth were successfully established in 15 of the mice. One mouse tumor showed early stalling in growth and was excluded from analysis. When tumors reached volume of approximately 100 mm^3 mice were treated with i.p. injection of di-scFv (40 mg/kg; $n = 8$) or an equivalent volume of control PBS ($n = 7$) weekly for 3 weeks. Tumor volumes and mouse body weights were tracked during the experiment, and at completion of the experiment mice were sacrificed and tumors were excised and masses recorded. All *in vivo* work was performed in accordance with institutional guidelines under an Institutional Animal Care and Use Committee-approved protocol.

Statistical analysis

P values were determined by the two-tailed Student *t* test. Error bars in figures represent SEM.

Results

Di-scFv is a divalent lupus anti-DNA autoantibody fragment

Di-scFv, composed of two scFv fragments linked in series, was generated to test our hypothesis that a larger, divalent 3E10 fragment with D31N mutations would have a more potent impact on BRCA2-deficient cancer cells compared with the original scFv. Schematics of scFv and di-scFv are shown in Fig. 1A and B. ScFv

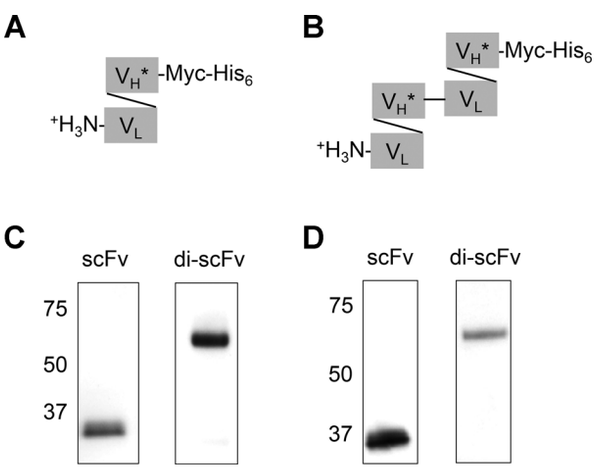

Figure 1.
Di-scFv. A and B, schematics of scFv (A) and di-scFv (B). V_L, variable region of the 3E10 light chain; V_H*, variable region of the 3E10 heavy chain with the enhancing D31N mutation in CDR1. C and D, purity and identity of scFv (molecular weight 30 kDa) and di-scFv (molecular weight 60 kDa) isolated from *P. pastoris* supernatant was confirmed by total protein stain (C) and anti-Myc Western blot analysis (D).

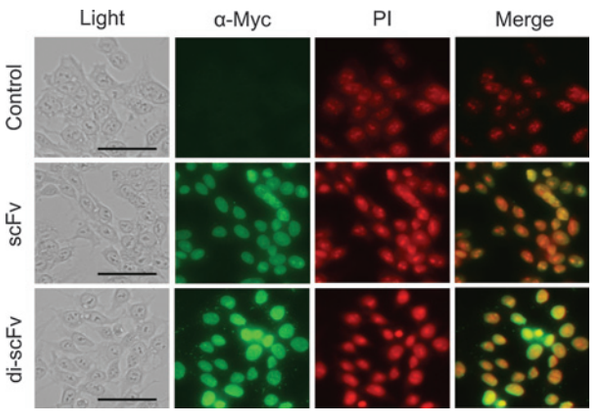

Figure 2.
Di-scFv penetrates cell nuclei. DLD1 cells treated with control buffer, scFv, or di-scFv were immunostained with an anti-Myc antibody to detect nuclear penetration by the 3E10 fragments. PI counterstain allows visualization of the nuclei. Both scFv and di-scFv colocalized with the PI nuclear stain, which confirms di-scFv retains the ability to penetrate cell nuclei; scale bar, 50 μm.

and di-scFv were produced in *P. pastoris*, and purified scFv and di-scFv were compared by SDS-PAGE and Western blot analysis. Di-scFv migrated at the expected molecular weight of 60 kDa, and Western blot analysis confirmed the presence of the C-terminal Myc tag, demonstrating that the protein was produced and purified in full-length form (Fig. 1C and D). To confirm that di-scFv retains the ability to penetrate into cell nuclei, DLD1 colon cancer cells were treated with control buffer or 5 μmol/L scFv or di-scFv for 1 hour. Cells were then washed, fixed, and immunostained for the C-terminal Myc tag in the 3E10 fragments. PI counterstain allowed direct visualization of the nucleus. Both scFv and di-scFv colocalized with the PI stain, demonstrating nuclear localization by both fragments (Fig. 2).

Di-scFv is more toxic to BRCA2-deficient cancer cells than scFv

The impact of scFv and di-scFv on the clonogenic survival of BRCA2-deficient CAPAN-1 cells was compared. CAPAN-1 cells were treated with scFv or di-scFv (0–6.6 μmol/L) and surviving fractions were determined by colony formation assay as previously described (1). Di-scFv was observed to be significantly more toxic to the CAPAN-1 cells than scFv (Fig. 3A). For example, at a dose as low as 0.8 μmol/L di-scFv reduced the surviving fraction of the cells to 0.51 ± 0.04, compared with 0.99 ± 0.13 with scFv ($P = 0.05$). At 6.6 μmol/L, di-scFv reduced the surviving fraction of the cells to 0.05 ± 0.02 compared with 0.20 ± 0.04 by scFv ($P = 0.03$). In these dose ranges the effect of di-scFv on the survival of the CAPAN-1 cells is similar to a previous report of the effect of PARP1 inhibition on CAPAN-1 cells (11).

To confirm that BRCA2 deficiency is associated with cellular sensitivity to di-scFv, we next compared the effects of scFv and di-scFv on the clonogenic survival of an isogenic pair of BRCA2-proficient and -deficient DLD1 colon cancer cells (12). The cells were treated with control media or 10 μmol/L scFv or di-scFv, and surviving fractions relative to control were determined by colony formation assay. As shown in Fig. 3B, neither scFv nor di-scFv were significantly toxic to the BRCA2-proficient cells (surviving fractions of 0.92 ± 0.05, $P = 0.1$, and 0.99 ± 0.06, $P = 0.6$, respectively), but both reduced the surviving fraction of the BRCA2-deficient cells (surviving fractions of 0.71 ± 0.06, $P = 0.006$, and 0.29 ± 0.09, $P = 0.007$, respectively). These data further demonstrate that di-scFv has a greater impact on BRCA2-deficient cancer cells than scFv and also show that di-scFv is not toxic to matched BRCA2-proficient cells.

Di-scFv is not toxic to MLH1-deficient cancer cells, but is synthetically lethal to PTEN-deficient U251 glioma cells

To further confirm that di-scFv is not simply universally cytotoxic, it was tested against additional cell lines. Specifically, H1975 lung cancer cells with intact DNA repair, SW48, and

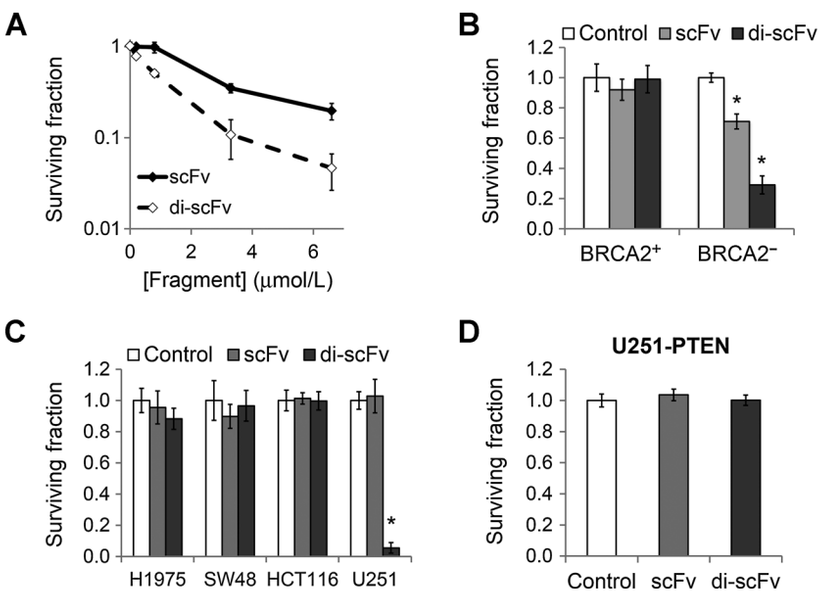

Figure 3.
Di-scFv has a potent impact on BRCA2- and PTEN-deficient cancer cells. A, BRCA2-deficient CAPAN-1 cells were treated with 0 to 6.6 μmol/L scFv or di-scFv and evaluated by colony formation assay. Di-scFv was significantly more toxic to the CAPAN-1 cells than scFv. B, an isogenic pair of $BRCA2^+$ and $BRCA2^-$ DLD1 cells was treated with control buffer or 10 μmol/L scFv or di-scFv, and surviving fractions were determined by colony formation assay. Neither scFv nor di-scFv was toxic to the $BRCA2^+$ cells. ScFv was mildly toxic to the $BRCA2^-$ cells (surviving fraction 0.71 ± 0.06), but di-scFv had a significantly greater impact (surviving fraction 0.29 ± 0.09); *, $P < 0.01$. C, DNA repair-proficient H1975, MLH1-deficient SW48 and HCT116, and PTEN-deficient U251 cells were treated with control buffer or 3.3 μmol/L scFv or di-scFv and evaluated by colony formation assay. ScFv was not significantly toxic to any of the cell lines, but di-scFv was highly toxic to the U251 cells; *, $P < 0.0001$. D, U251-PTEN cells were treated with control buffer or 3.3 μmol/L scFv or di-scFv, and surviving fractions were determined by clonogenic assay. Di-scFv was not toxic to the U251-PTEN cells, indicating that PTEN status is associated with sensitivity to di-scFv.

HCT116 colon cancer cells with defective DNA mismatch repair due to MLH1 deficiency, and U251 glioma cells were treated with control media or media containing 3.3 μmol/L scFv or di-scFv, and surviving fractions were determined by colony formation assay. As expected, neither fragment was significantly toxic to the H1975 cells that have intact DNA repair mechanisms. Similarly, neither fragment had any significant impact on survival of the MLH1-deficient SW48 and HCT116 cells, indicating that mismatch repair defects do not confer sensitivity to the fragments. Consistent with our previous results, scFv was not toxic to the U251 cells (1). However, di-scFv was highly toxic to the U251 cells, with surviving fraction reduced to 0.06 ± 0.03 ($P < 0.0001$; Fig. 3C). The large impact of di-scFv on the U251 cells was somewhat surprising, particularly given that the scFv had no detectable impact on the cells. However, U251 glioma cells are known to be PTEN-deficient, and an association between PTEN status and HDR efficiency has been suggested (13–15). In addition, the observed effect of di-scFv on U251 cell survival is comparable with the previously reported impact of the PARP1 inhibitor olaparib on U251 cells (16). We hypothesized that PTEN deficiency was responsible for the observed sensitivity to di-scFv, and to confirm this, we obtained matched PTEN-proficient U251 cells (U251-PTEN) and tested their sensitivity to 3.3 μmol/L di-scFv. As shown in Fig. 3D, the U251-PTEN cells were not sensitive to di-scFv. To the best of our knowledge, this is the first evidence to suggest synthetic lethality resulting from exposure of PTEN-deficient cancer cells to a lupus autoantibody fragment.

Di-scFv causes accumulation of DNA DSBs in PTEN- and BRCA2-deficient cancer cells

BRCA2 deficiency is well known to result in defective HDR and to confer sensitivity to inhibition of both DNA single- and double-strand break repair mechanisms. The details of the association between PTEN status and efficiency of HDR are less clear, but several groups have reported impaired HDR in and increased sensitivity of PTEN-deficient cells to genotoxic stress and to inhibition of PARP1 (13, 14, 17–19). We therefore hypothesized that the reason the PTEN- and BRCA2-deficient cells exhibit increased sensitivity to di-scFv compared with scFv is that the increased avidity and larger size of di-scFv yields greater inhibition of DSB repair and accumulation of DNA DSBs in these cells. To test this hypothesis U251 cells were treated with control media or 25 μmol/L scFv or di-scFv for 4 or 24 hours, and the number of DNA DSBs present were visualized by immunostaining for γH2AX foci. ScFv did not yield any increase in γH2AX foci at either time point, with 11.7 ± 1.3 and 11.2 ± 1.0 mean foci per cell in control cells at 4 and 24 hours, respectively, compared with 11.7 ± 1.2 and 8.8 ± 0.8 mean foci per cell in cells treated with scFv. Di-scFv similarly did not significantly increase the mean foci per cell after 4 hours of exposure (13.8 ± 1.5 mean foci per cell, $P = 0.27$), but 24 hours of exposure to di-scFv increased the mean number of foci per cell to 25.1 ± 1.2 ($P < 0.0001$), which is consistent with a time-dependent accumulation of DNA DSBs due to inhibition of BER and HDR in these PTEN-deficient cells (Fig. 4A and B). By contrast, 24 hours of exposure to di-scFv did not cause any significant increase in γH2AX foci in PTEN-proficient U251-PTEN cells (11.2 ± 1.1 mean foci per cell in control cells compared with 13.7 ± 1.2 and 11.7 ± 1.2 in cells treated with scFv and di-scFv, respectively; Fig. 4C). The impact of di-scFv on γH2AX foci in BRCA2-deficient CAPAN-1 cells was also evaluated, and as expected 24 hours of exposure to di-scFv resulted in a significant increase in the numbers of γH2AX foci (14.9 ± 2.0 foci in cells treated with di-scFv compared with 9.3 ± 1.8 foci in control cells; $P = 0.04$; Fig. 4D and E).

p53-binding protein 1 (53BP1) is phosphorylated in response to DNA damage and recruited to sites of DNA DSBs, and as a second test to confirm that di-scFv yields an increase in DNA DSBs in PTEN-deficient cells, we evaluated the effect of di-scFv on phospho-53BP1 foci in the U251 and U251-PTEN cells. The matched pair of cells was treated for 24 hours with control media or 20 μmol/L di-scFv and then phospho-53BP1 foci were visualized by immunofluorescence. Consistent with the results

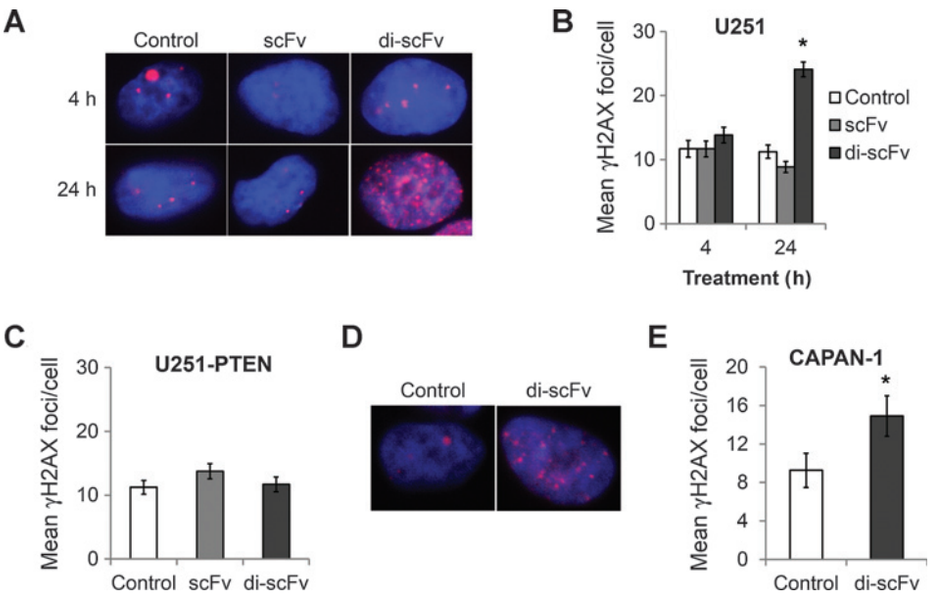

Figure 4.
Di-scFv causes accumulation of γH2AX foci in PTEN- and BRCA2-deficient cancer cells. A and B, PTEN-deficient U251 cells were treated with control media or 25 μmol/L scFv or di-scFv for 4 or 24 hours, and γH2AX foci were then visualized by immunofluorescence. Example cell images are shown in A and mean number of foci per cell is presented in B. *, $P < 0.0001$. C, U251-PTEN cells were treated with control media or 25 μmol/L scFv or di-scFv for 24 hours, and γH2AX foci were then visualized by immunofluorescence and mean number of foci per cell was determined. D and E, BRCA2-deficient CAPAN-1 cells were treated with control buffer or 25 μmol/L di-scFv for 24 hours, and γH2AX foci were then visualized by immunofluorescence. Example cell images are shown in D, and mean number of foci per cell is presented in E. *, $P = 0.04$.

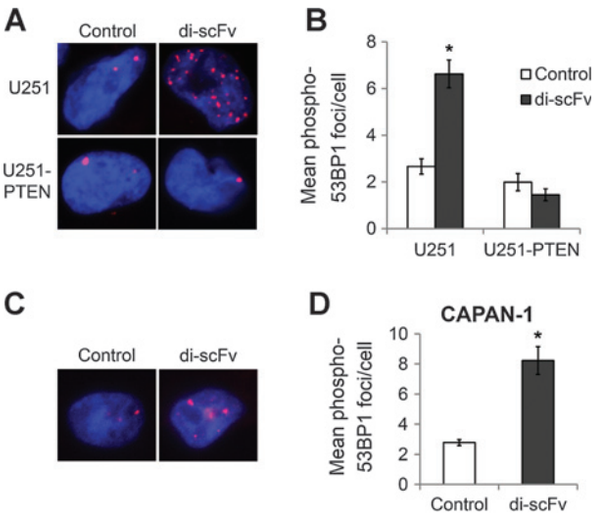

Figure 5.
Di-scFv causes accumulation of phospho-53BP1 foci in PTEN- and BRCA2-deficient cancer cells. A and B, U251 and U251-PTEN cells were treated with control media or 20 μmol/L di-scFv for 24 hours and then immunostained for phospho-53BP1. Example cell images are shown in A and mean number of foci per cell is presented in B. *, $P < 0.0001$. C and D, BRCA2-deficient CAPAN-1 cells were treated with control buffer or 4.4 μmol/L di-scFv for 24 hours and then immunostained for phospho-53BP1. Example cell images are shown in C, and mean number of foci per cell is presented in D; *, $P < 0.001$.

obtained in the γH2AX assay, di-scFv significantly increased the mean number of phospho-53BP1 foci in the U251 cells to 6.6 ± 0.6 compared with 2.7 ± 0.3 in control cells ($P < 0.0001$), but did not increase the number of foci in the U251-PTEN cells (1.5 ± 0.4 foci in control cells and 1.5 ± 0.3 foci in cells treated with di-scFv, $P = 0.2$; Fig. 5A and B). As expected, 24 hours of exposure to di-scFv also increased the number of phospho-53BP1 foci in BRCA2-deficient CAPAN-1 cells to 8.2 ± 0.9 compared with 2.8 ± 0.2 in control cells ($P < 0.001$; Fig. 5C and D). Taken together, the results from the γH2AX and phospho-53BP1 assays suggest that inhibition of DNA repair by di-scFv is not sufficient to cause accumulation of DNA DSBs in cells with intact HDR, but does result in accumulation of such damage in cells with defects in HDR associated with BRCA2 or PTEN deficiency. We believe the accumulation of DNA DSBs caused by di-scFv in the BRCA2- and PTEN-deficient cancer cells is responsible for its selective impact on the clonogenic survival of these cells.

Di-scFv suppresses the growth of BRCA2-deficient tumors *in vivo*

The effect of 3E10 on BRCA2-deficient tumors has not previously been tested *in vivo*, primarily because the modest effect of the original antibody on BRCA2-deficient cells in culture was not considered sufficient to be likely to yield an observable impact on gross tumors. However, as detailed above di-scFv exhibited potent toxicity to BRCA2-deficient cancer cells, and we therefore hypothesized that di-scFv would be able to yield detectable suppression of the growth of BRCA2-deficient tumors *in vivo*, and thereby provide proof of principle for the use of a lupus autoantibody fragment as a single-agent against BRCA2-deficient tumors. BRCA2-deficient CAPAN-1 subcutaneous xenografts were generated in immunodeficient mice, and when tumors reached size of approximately 100 mm^3 the mice were treated with three weekly i.p. injections of control buffer or di-scFv (40 mg/kg). Tumor volumes were followed and masses were recorded at the end of the experiment. As predicted, di-scFv significantly suppressed the growth of the tumors, evidenced by decreased tumor volumes and masses (Fig. 6A and B). For example, at the midpoint of the experiment (2 weeks after the first treatment) mean tumor volume in mice treated with control buffer was 476 ± 54 mm^3 compared with 277 ± 29 mm^3 in mice treated with di-scFv ($P = 0.005$). At the end of the experiment (4 weeks after the first treatment) mean tumor volume in mice treated with control buffer was 1,102 ± 235 mm^3 compared with 606 ± 57 mm^3 in mice treated with di-scFv ($P = 0.05$; Fig. 6A). Mean tumor mass at the end of the experiment in mice treated with control buffer was 0.73 ± 0.2 g compared with 0.33 ± 0.03 g in mice treated with di-scFv ($P = 0.03$; Fig. 6B). Di-scFv was well tolerated by the mice with no observable toxicities. Mean body weights were indistinguishable between the mice treated with control buffer or di-scFv (Fig. 6C). To the best of our knowledge, this is the first demonstration of suppression of growth of an HDR-deficient tumor by a lupus autoantibody fragment.

Discussion

Tumor-specific targets sequestered inside cells and nuclei are inaccessible to most antibodies, which has been a limiting factor in antibody-based cancer therapy. Only seven antibodies are presently FDA approved for the treatment of solid tumors,

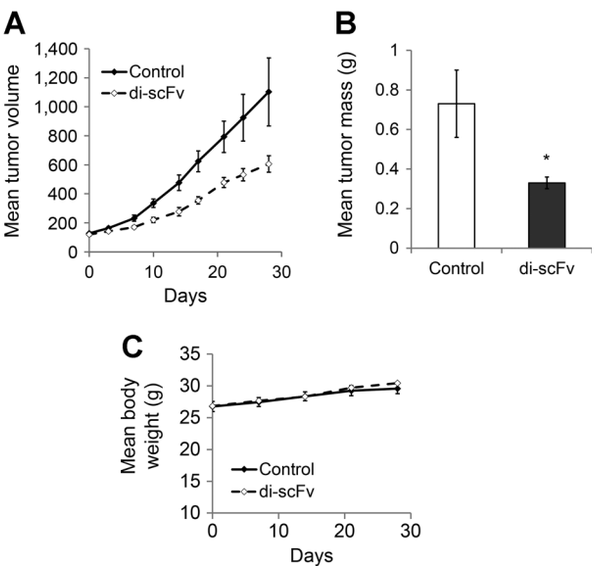

Figure 6.
Di-scFv suppresses the growth of BRCA2$^-$ CAPAN-1 pancreatic tumors *in vivo*. CAPAN-1 subcutaneous xenografts were generated in nude mice, and when tumors reached volumes of approximately 100 mm^3, mice were treated with weekly i.p. injections of control buffer or di-scFv (40 mg/kg) for 3 weeks (day 0 represents first treatment date). Tumor growth curves are shown in A, and tumor masses measured at the end of the experiment (day 28 after treatment) are shown in B. Di-scFv significantly suppressed the growth of the tumors (*, $P = 0.03$) but was not toxic to the mice. C, mouse body weights were recorded throughout the *in vivo* tumor growth suppression experiment, and no distinguishable differences between control and experimental groups were observed.

and all target extracellular antigens (EGFR, HER2, CTLA-4, or VEGF; ref. 20). The use of the cell-penetrating lupus autoantibody 3E10 to selectively affect cancer cells is a new approach. 3E10 penetrates cells through an equilibrative nucleoside transporter (ENT2) that is expressed in nearly all cells (9), and once inside the nucleus 3E10 appears to incompletely inhibit BER and HDR, which is not toxic to normal cells, but is synthetically lethal to cells that have preexisting defects in HDR due to BRCA2 deficiency (1). The targeted effect of 3E10 and its fragments on HDR-deficient cancer cells, therefore, is not necessarily due to selective penetration into cancer cells, but rather to the selective sensitivity of HDR-deficient cancer cells to further inhibition of DNA repair by 3E10. This is markedly distinct from nonpenetrating antibodies that target cancer cells by recognizing and binding to antigens that are overexpressed on the surface of certain cancer cells (20).

A further difference between 3E10 and nonpenetrating antibodies relates to respective methods of tumor toxicity. Nonpenetrating antibodies such as cetuximab that target extracellular receptors depend in part on Fc-mediated activation of ADCC and complement to exert an effect on tumors, and elimination of the Fc, therefore, diminishes the magnitude of their effect (21). By contrast, the ability of 3E10 to penetrate nuclei, bind DNA and inhibit DNA repair, and exert a synthetically lethal effect on BRCA2-deficient cells is independent of the 3E10 Fc region (1). This important difference between 3E10 and other antibodies is the primary reason that we have focused our efforts on optimizing 3E10 fragments that lack an Fc region for cancer therapy rather than making adjustments to the full 3E10 antibody. Specifically, 3E10 fragments that lack an Fc should be unable to activate ADCC and complement, and therefore will carry a lower risk of nonspecific side effects in clinical trials that may be considered in the reasonably near future.

As described above, even at high doses the magnitude of inhibition of DNA repair by scFv results in only a modest effect on cancer cells with defective HDR (1), and therefore the potential to use scFv by itself as a therapeutic agent targeted against HDR-deficient tumors is limited. However, we have now shown that di-scFv, a divalent 3E10 fragment with enhancing D31N mutations, has a greater effect on HDR-deficient cancer cells, but still remains nontoxic to cells with intact HDR. The increased potency of di-scFv is likely related to increased avidity for DNA due to its second binding site. The larger size of di-scFv also provides further advantages over scFv, including likely greater steric hindrance of DNA repair factors, decreased renal filtration *in vivo* and therefore a longer circulating half-life, and increased accumulation in tumor tissue due to the enhanced permeability and retention phenomenon (22, 23).

Another important finding that has emerged from the present study is an apparent association between PTEN deficiency and sensitivity to di-scFv. PTEN is linked to numerous cellular functions, including AKT signaling, cell-cycle regulation, HDR, and maintenance of genomic integrity (13, 15, 19, 24–26). We have previously shown that 3E10 inhibits BER and HDR, and have now found that di-scFv causes a selective increase in DSBs in PTEN-deficient cells. Taken together, these findings are most consistent with a preexisting impairment in DNA DSB repair in the PTEN-deficient cells, likely related to defective HDR, being responsible for their sensitivity to di-scFv. PTEN deficiency is associated with many malignancies, including breast, prostate, glioma, ovarian, endometrial, melanoma, and lung cancers (15, 27–33). Additional studies are needed to fully explore the potential to use di-scFv against PTEN-deficient tumors, but the finding that PTEN deficiency may be predictive of sensitivity to di-scFv significantly increases the number of malignancies that may be susceptible to 3E10-based therapy. Of note, di-scFv was highly toxic to the PTEN-deficient U251 cells at a dose of 3.3 μmol/L, whereas scFv had no effect on the survival of the cells at the same dose. In addition, we have previously shown that scFv is not toxic to the U251 cells even at a dose of 10 μmol/L (1), which is approximately three times the dose at which di-scFv was observed to have a significant effect on the cells. These data, therefore, further suggest that the greater potency of di-scFv is related to increased avidity for DNA, and that the effectiveness of di-scFv cannot be matched by simply doubling the dose of scFv.

Most importantly, in the present study, we have confirmed that the enhanced potency of di-scFv is preserved *in vivo* by showing that di-scFv by itself yields measurable and significant suppression of the growth of BRCA2-deficient CAPAN-1 tumors. To the best of our knowledge, this is the first demonstration of an effect of a lupus autoantibody fragment on DNA repair-deficient tumors *in vivo*, and these data, therefore, provide strong support for continuing studies into the potential applications of lupus autoantibodies and derivatives thereof in cancer therapy. Efforts to scale up production of di-scFv for testing against a wide range of HDR-deficient tumors and in greater numbers of animals are currently underway, and we are optimistic that further optimizations will yield 3E10-based therapeutics with even greater potential clinical utility.

Disclosure of Potential Conflicts of Interest

G. Chan, R.H. Weisbart, and J.E. Hansen have ownership interest (including patents) as inventors on Yale University patent filing "Cell-penetrating anti-DNA antibodies and uses thereof to inhibit DNA repair." No potential conflicts of interest were disclosed by the other authors.

Authors' Contributions

Conception and design: G. Chan, R.H. Weisbart, J.E. Hansen
Development of methodology: P.W. Noble, R.H. Weisbart, J.E. Hansen
Acquisition of data (provided animals, acquired and managed patients, provided facilities, etc.): P.W. Noble, J.E. Hansen
Analysis and interpretation of data (e.g., statistical analysis, biostatistics, computational analysis): P.W. Noble, J.E. Hansen
Writing, review, and/or revision of the manuscript: P.W. Noble, M.R. Young, J.E. Hansen
Administrative, technical, or material support (i.e., reporting or organizing data, constructing databases): P.W. Noble, G. Chan, M.R. Young
Study supervision: J.E. Hansen
Other (developed the molecular construct used in these studies): R.H. Weisbart

Grant Support

This work was supported by the Department of Therapeutic Radiology at Yale School of Medicine (J.E. Hansen) and a Veterans Affairs Merit Review grant (R.H. Weisbart). J.E. Hansen was also supported in part by a Research Scholar Grant from the Radiological Society of North America.

The costs of publication of this article were defrayed in part by the payment of page charges. This article must therefore be hereby marked *advertisement* in accordance with 18 U.S.C. Section 1734 solely to indicate this fact.

Received August 1, 2014; revised March 1, 2015; accepted March 4, 2015; published OnlineFirst April 1, 2015.

References

1. Hansen JE, Chan G, Liu Y, Hegan DC, Dalal S, Dray E, et al. Targeting cancer with a lupus autoantibody. Sci Trans Med 2012;4:157ra42.
2. Weisbart RH, Stempniak M, Harris S, Zack DJ, Ferreri K. An autoantibody is modified for use as a delivery system to target the cell nucleus: therapeutic implications. J Autoimmun 1998;11:539–46.
3. Weisbart RH, Hansen JE, Chan G, Wakelin R, Chang SS, Heinze E, et al. Antibody-mediated transduction of p53 selectively kills cancer cells. Int J Oncol 2004;25:1867–73.
4. Rudnick SI, Adams GP. Affinity and avidity in antibody-based tumor targeting. Cancer Biother Radiopharm 2009;24:155–61.
5. Beckman RA, Weiner LM, Davis HM. Antibody constructs in cancer therapy: protein engineering strategies to improve exposure in solid tumors. Cancer 2007;109:170–9.
6. King DJ, Turner A, Farnsworth AP, Adair JR, Owens RJ, Pedley RB, et al. Improved tumor targeting with chemically cross-linked recombinant antibody fragments. Cancer Res 1994;54:6176–85.
7. Weisbart RH, Wakelin R, Chan G, Miller CW, Koeffler PH. Construction and expression of a bispecific single-chain antibody that penetrates mutant p53 colon cancer cells and binds p53. Int J Oncol 2004;25:1113–8.
8. Hansen JE, Sohn W, Kim C, Chang SS, Huang NC, Santos DG, et al. Antibody-mediated Hsp70 protein therapy. Brain Res 2006;1088:187–96.
9. Hansen JE, Tse CM, Chan G, Heinze ER, Nishimura RN, Weisbart RH. Intranuclear protein transduction through a nucleoside salvage pathway. J Biol Chem 2007;282:20790–3.
10. Zhan X, Ander BP, Liao IH, Hansen JE, Kim C, Clements D, et al. Recombinant Fv-Hsp70 protein mediates neuroprotection after focal cerebral ischemia in rats. Stroke 2010;41:538–43.
11. Porcelli L, Quatrale AE, Mantuano P, Leo MG, Silvestris N, Rolland JF, et al. Optimize radiochemotherapy in pancreatic cancer: PARP inhibitors a new therapeutic opportunity. Mol Oncol 2013;7:308–22.
12. Hucl T, Rago C, Gallmeier E, Brody JR, Gorospe M, Kern SE. A syngeneic variance library for functional annotation of human variation: application to BRCA2. Cancer Res 2008;68:5023–30.
13. McEllin B, Camacho CV, Mukherjee B, Hahm B, Tomimatsu N, Bachoo RM, et al. PTEN loss compromises homologous recombination repair in astrocytes: implications for glioblastoma therapy with temozolomide or poly(ADP-ribose) polymerase inhibitors. Cancer Res 2010;70:5457–64.
14. Mendes-Pereira AM, Martin SA, Brough R, McCarthy A, Taylor JR, Kim JS, et al. Synthetic lethal targeting of PTEN mutant cells with PARP inhibitors. EMBO Mol Med 2009;1:315–22.
15. Bassi C, Ho J, Srikumar T, Dowling RJ, Gorrini C, Miller SJ, et al. Nuclear PTEN controls DNA repair and sensitivity to genotoxic stress. Science 2013;341:395–9.
16. Irwin CP, Portorreal Y, Brand C, Zhang Y, Desai P, Salinas B, et al. PARPi-FL—a fluorescent PARP1 inhibitor for glioblastoma imaging. Neoplasia 2014;16:432–40.
17. Dedes KJ, Wetterskog D, Mendes-Pereira AM, Natrajan R, Lambros MB, Geyer FC, et al. PTEN deficiency in endometrioid endometrial adenocarcinomas predicts sensitivity to PARP inhibitors. Sci Trans Med 2010;2:53ra75.
18. Forster MD, Dedes KJ, Sandhu S, Frentzas S, Kristeleit R, Ashworth A, et al. Treatment with olaparib in a patient with PTEN-deficient endometrioid endometrial cancer. Nat Rev Clin Oncol 2011;8:302–6.
19. Puc J, Parsons R. PTEN loss inhibits CHK1 to cause double stranded-DNA breaks in cells. Cell Cycle 2005;4:927–9.
20. Scott AM, Wolchok JD, Old LJ. Antibody therapy of cancer. Nat Rev Cancer 2012;12:278–87.
21. Kellner C, Derer S, Valerius T, Peipp M. Boosting ADCC and CDC activity by Fc engineering and evaluation of antibody effector functions. Methods 2014;65:105–13.
22. Jang SH, Wientjes MG, Lu D, Au JL. Drug delivery and transport to solid tumors. Pharm Res 2003;20:1337–50.
23. Maeda H, Wu J, Sawa T, Matsumura Y, Hori K. Tumor vascular permeability and the EPR effect in macromolecular therapeutics: a review. J Control Release 2000;65:271–84.
24. Gupta A, Yang Q, Pandita RK, Hunt CR, Xiang T, Misri S, et al. Cell-cycle checkpoint defects contribute to genomic instability in PTEN deficient cells independent of DNA DSB repair. Cell Cycle 2009;8:2198–210.
25. Radu A, Neubauer V, Akagi T, Hanafusa H, Georgescu MM. PTEN induces cell-cycle arrest by decreasing the level and nuclear localization of cyclin D1. Mol Cell Biol 2003;23:6139–49.
26. Shen WH, Balajee AS, Wang J, Wu H, Eng C, Pandolfi PP, et al. Essential role for nuclear PTEN in maintaining chromosomal integrity. Cell 2007;128:157–70.
27. Kane MF, Loda M, Gaida GM, Lipman J, Mishra R, Goldman H, et al. Methylation of the hMLH1 promoter correlates with lack of expression of hMLH1 in sporadic colon tumors and mismatch repair-defective human tumor cell lines. Cancer Res 1997;57:808–11.
28. Vlietstra RJ, van Alewijk DC, Hermans KG, van Steenbrugge GJ, Trapman J. Frequent inactivation of PTEN in prostate cancer cell lines and xenografts. Cancer Res 1998;58:2720–3.
29. Steck PA, Pershouse MA, Jasser SA, Yung WK, Lin H, Ligon AH, et al. Identification of a candidate tumour suppressor gene, MMAC1, at chromosome 10q23.3 that is mutated in multiple advanced cancers. Nat Genet 1997;15:356–62.
30. Li J, Yen C, Liaw D, Podsypanina K, Bose S, Wang SI, et al. PTEN, a putative protein tyrosine phosphatase gene mutated in human brain, breast, and prostate cancer. Science 1997;275:1943–7.
31. Cancer Genome Atlas Research N. Comprehensive genomic characterization defines human glioblastoma genes and core pathways. Nature 2008;455:1061–8.
32. Cancer Genome Atlas Research N. Integrated genomic analyses of ovarian carcinoma. Nature 2011;474:609–15.
33. Mutter GL, Lin MC, Fitzgerald JT, Kum JB, Baak JP, Lees JA, et al. Altered PTEN expression as a diagnostic marker for the earliest endometrial precancers. J Natl Cancer Inst 2000;92:924–30.